

# Active-Site-Accessible, Porphyrinic Metal–Organic Framework Materials

Omar K. Farha,\* Abraham M. Shultz, Amy A. Sarjeant, SonBinh T. Nguyen,\* and Joseph T. Hupp\*

Department of Chemistry and the Institute for Catalysis in Energy Processes, Northwestern University, 2145 Sheridan Road, Evanston, Illinois 60208, United States

**S** Supporting Information

**ABSTRACT:** On account of their structural similarity to cofactors found in many metallo-enzymes, metalloporphyrins are obvious potential building blocks for catalytically active, metal–organic framework (MOF) materials. While numerous porphyrin-based MOFs have already been described, versions featuring highly accessible active sites and permanent microporosity are remarkably scarce. Indeed, of the more than 70 previously reported porphyrinic MOFs, *only one* has been shown to be both permanently microporous and contain internally accessible active sites for chemical catalysis. Attempts to generalize the design approach used in this single successful case have failed. Reported here, however, is the synthesis of an extended family of MOFs that directly incorporate a variety of metalloporphyrins (specifically  $\text{Al}^{3+}$ ,  $\text{Zn}^{2+}$ ,  $\text{Pd}^{2+}$ ,  $\text{Mn}^{3+}$ , and  $\text{Fe}^{3+}$  complexes). These robust porphyrinic materials (RPMs) feature large channels and readily accessible active sites. As an illustrative example, one of the manganese-containing RPMs is shown to be catalytically competent for the oxidation of alkenes and alkanes.

The already sizable field of metal–organic framework (MOF) chemistry continues to expand at a remarkable pace,<sup>1</sup> in part because of the seemingly limitless number of potential structures, but also because of myriad potential applications.<sup>2</sup> Prominent among these applications is chemical catalysis.<sup>3</sup> Like zeolites (by far the most widely used catalysts industrially) MOFs promise catalysis-friendly features such as large internal surface areas, extensive micro- and/or mesoporosity, and crystallographically well-defined cavities and portals of molecular dimensions. In addition, because they enlist the chemistry of carbon they offer enormous tunability with respect to chemical functionality and composition. One attractive approach to the construction of catalytic MOFs, therefore, is to incorporate as struts (or less commonly, as nodes) molecules that have already been proven effective as catalysts in homogeneous solution environments. Examples include metallo-salens<sup>4</sup> and Ti-BINOLate complexes.<sup>5</sup>

Also seemingly attractive would be MOFs containing metalloporphyrins, as metalated porphyrins and their congeners are ubiquitous in metallo-enzymology, functioning, for example, as the key active sites in a range of oxidases,<sup>6</sup> peroxidases,<sup>6</sup> isomerases,<sup>7</sup> dehalogenases,<sup>7</sup> and transferases.<sup>7</sup> Indeed, one of the earliest intentional attempts (Robson and co-workers) to create a crystalline and permanently microporous MOF utilized copper porphyrins as building blocks.<sup>8</sup> While no catalytic studies were described, the report emphasized the *potential* of metallo-porphyrinic MOFs as catalysts. Since then, 74 additional two- or three-dimensional porphyrinic MOFs have been described (see Supporting

Information (SI) for complete references). Remarkably, and despite considerable effort, only one has been shown to be both catalytically competent and porous with respect to chemical reactants.<sup>9</sup>

The problems encountered in building robust, catalytic MOFs from porphyrins have been several. In the early report from Robson, large cavities and pores were obtained, but the framework irreversibly collapsed upon removal of solvent.<sup>8,10</sup> Fortunately, a recently described “activation” strategy involving solvent exchange with liquid  $\text{CO}_2$ , followed by supercritical drying,<sup>11</sup> has proven effective in preventing the collapse of a variety of MOFs having high initial solvent content.<sup>12</sup> Several years after Robson’s report, Suslick and co-workers<sup>13</sup> succeeded in using 5,10,15,20-tetrakis(4-carboxyphenyl)porphyrin to build zeolite structural analogues from cobalt and manganese salts (PIZA series). The Co(porphyrin)-based PIZA-1 showed remarkable size selectivity with respect to small-molecule sorption (water, methanol, ethanol, 1-butylamine, among others), and the Mn(porphyrin)-based PIZA-3 was shown to be capable of oxidative catalysis. However, these materials feature very small channels, and the authors concluded that catalysis of the substrates examined (larger than those used for sorption studies with PIZA-1) occurs only on the exterior surface. Choe and co-workers<sup>14</sup> have used a paddlewheel coordination motif with the same tetracarboxylate porphyrin to construct 2D metal–organic sheets that are pillared in the third dimension by dipyriddy struts.<sup>15</sup> While these materials are permanently microporous, unfortunately the metal ions in the porphyrin struts behave as structural nodes, preventing their use as catalysts. (Exceptions are MOFs constructed from Pd(II)porphyrins. The Pd(II) ions, however, are coordinatively saturated by the porphyrin itself, so lack affinity for candidate substrate molecules.<sup>15</sup>) Similar active-site blocking has been encountered in several other studies.<sup>16</sup>

Finally, also of interest is a very recent report by Choe and co-workers on the use of 2,2'-methyl-4,4'-bipyridine as a pillaring strut.<sup>17</sup> The methyl substituents were intended to prevent coordination of the strut at the porphyrinic metal site, while still allowing for coordination by metal ions contained in the paddlewheel nodes. Single-crystal X-ray structural studies show that this clever approach indeed does work, in the sense that the desired control over pillar coordination is achieved. Unfortunately, the evacuated compounds showed almost no accessible internal surface area (81  $\text{m}^2/\text{g}$  based on  $\text{CO}_2$  adsorption), implying framework collapse.<sup>18,19</sup>

We have recently succeeded in building a noninterpenetrated, pillared-paddlewheel MOF by combining 1,2,4,5-tetrakis(4-carboxyphenyl)benzene and 5,15-dipyriddy-10,20-bis(pentafluorophenyl)-porphyrin with a Zn salt. This crystalline compound (**ZnPO-MOF**)

**Received:** December 8, 2010

**Published:** March 29, 2011

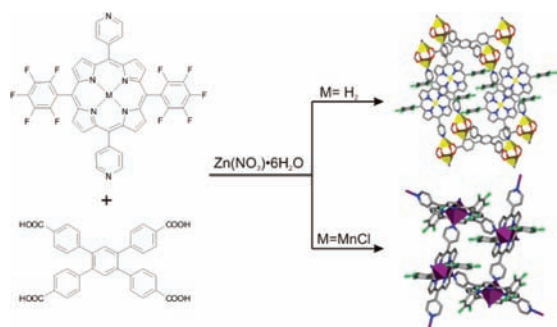


**Figure 1.** Using the free-base dipyriddy porphyrin, the highly porous Zn(porphyrin)-based material **ZnPO-MOF** can be easily synthesized (top right). However, starting with the Mn(porphyrin) yields only a 2D material (bottom right), in which the Mn in the porphyrin center acts as a structural node (and the tetrapotic carboxylate strut is not incorporated). The coordinatively saturated metal center of the 2D material is useless for catalysis.

featured a high degree of porosity and contained fully reactant-accessible metalloporphyrin sites.<sup>9</sup> Remarkably, despite extensive prior synthesis efforts, **ZnPO-MOF** was the first metalloporphyrin-based MOF to show catalytic activity in the interior of the material. Unfortunately, our attempts to extend the approach to catalytically more interesting metals such as Fe(III) were uniformly unsuccessful. For example, efforts to employ other metallo-porphyrins as building blocks for catalytic MOFs were undermined by the propensity of these components to form instead networks in which the intended active site serves as an auxiliary node. Figure 1 shows an example involving a Mn(III)porphyrin as a building block. A second tack involved efforts to prepare a free-base analogue of the previously synthesized catalytic MOF, with the aim of *postsynthetically* metallating it. These efforts were thwarted by the effectiveness of the porphyrin in sequestering zinc ions that we hoped instead would form framework nodes. (It is worth noting an alternative approach by Eddaoudi and co-workers.<sup>20</sup> They electrostatically encapsulated free, cationic metalloporphyrins within cavities of anionic MOFs.)

In this report, we describe the successful synthesis of MOFs that can incorporate a variety of metalloporphyrins (specifically  $\text{Al}^{3+}$ ,  $\text{Zn}^{2+}$ ,  $\text{Pd}^{2+}$ ,  $\text{Fe}^{3+}$ , and  $\text{Mn}^{3+}$  complexes) as components of well-defined, crystalline, highly porous, and stable materials. These robust porphyrinic materials (**RPMs**) are effective catalysts for the oxidation of alkenes and alkanes and are highly stable under oxidative conditions in comparison to homogeneous catalyst analogues.

Due to the tendency of catalytically interesting metals to favor penta- or hexa-coordination, the synthesis of MOFs with available Fe- or Mn-porphyrin sites has not been straightforward until now. As noted above, simply targeting pillared paddlewheel MOFs with metalloporphyrin struts typically results in ligation of both the paddlewheel and porphyrin metal sites. Our synthetic approach employed two strategies to avoid this problem. First, we took advantage of the steric bulk to create a structure with as few pillars as possible. This was accomplished by using a tetracarboxylated porphyrin ligand ( $\text{L}^1$ ) in conjunction with a bulky dipyriddy porphyrin pillar ( $\text{L}^2$ ). The building block  $\text{L}^2$  was chosen, in part, because of the known ability of electron-withdrawing groups such as fluorine to greatly increase the activity of metalloporphyrins for oxidative catalysis.<sup>21</sup> We have previously shown that the use of tetracarboxylated ligands can produce MOFs particularly sensitive to sterics, producing noninterpenetrated structures.<sup>22</sup> Here, the steric bulk prevents pillar coordination at the metalloporphyrin site. The second element of our approach was to exploit differences in solubility of the

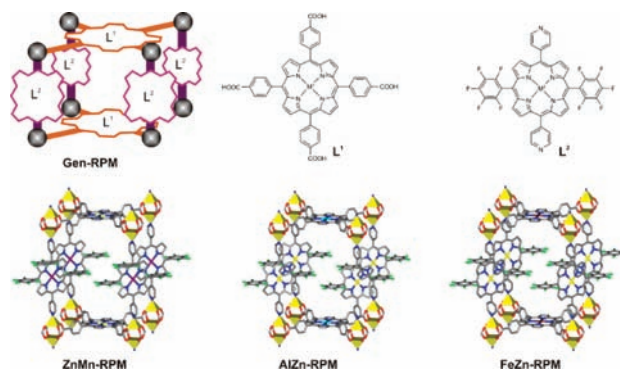


**Figure 2.** Structure of **RPM** materials. Top left: A schematic representation of a generic **RPM** unit cell, based on sheet formation by the tetraacid ligand ( $\text{L}^1$ ) pillaring by a dipyriddy strut ( $\text{L}^2$ ). The gray-black spheres are the paddlewheel-coordinated zinc nodes. Top center and right: Structures of the porphyrinic struts used to synthesize the **RPM** series ( $\text{M}^1 = 2\text{H}$ , Pd, Al(OH) or Fe(Cl),  $\text{M}^2 = 2\text{H}$  or Mn(Cl)); Bottom: Crystallography-derived stick representations of the unit cells of three representative **RPMs** (yellow polyhedra = Zn, yellow = Zn, brown = Fe, purple = Mn, teal = Al, red = O, green = F, blue = N, gray = C, white = H). Hydrogen atoms and disordered solvent molecules have been omitted for clarity.

carboxylate- and pyridyl-porphyrin struts. By using a solvent mixture (1:1 v/v DMF/EtOH) in which the tetracarboxylate has good solubility, and the dipyriddy has poor, the growing 2D metal/carboxylate sheets have access to a low effective concentration of the dipyriddy subunit. This results in pillar coordination only at the more favorable sites, i.e. paddlewheel sites.

With the aforementioned strategies in mind, we found that static heating of  $\text{L}^1$  and  $\text{Zn}(\text{NO}_3)_2 \cdot 6\text{H}_2\text{O}$  in DMF at 80 °C for 2 h, followed by addition of 0.03 M  $\text{HNO}_3$  in ethanol and  $\text{L}^2$  and heating of the resulting suspension at 80 °C for 20 h, resulted in the formation of block-shaped crystals, suitable for single-crystal X-ray diffraction. The sequence of ligand addition is important; suitable materials are not obtained if the order is reversed. We speculate that delaying the addition of the dipyriddy strut until *after* the tetracarboxylate strut has begun to assemble with zinc ions (as coordinatively unsaturated nodes) prevents the formation of 2D aggregates of the dipyriddy unit. Several isostructural materials were made in which the metals in  $\text{L}^2$  and  $\text{L}^1$  were varied (Figure 2).  $\text{L}^1$  was employed as an  $\text{Al}^{3+}$ ,  $\text{Pd}^{2+}$ , or  $\text{Fe}^{3+}$  complex, or simply as a free-base porphyrin, while  $\text{L}^2$  was used as either the  $\text{Mn}^{3+}$  complex or the free-base. For both kinds of struts, use of a free-base porphyrin in the synthesis resulted in  $\text{Zn}^{2+}$  complexes in the **RPM**. Analysis of single-crystal data revealed noncatenated frameworks with formula of  $\text{Zn}_2(\text{L}^1)(\text{L}^2)$ . As expected,  $\text{L}^1$  bridges the  $\text{Zn}^{\text{II}}$  dimers and forms flat two-dimensional sheets that are, indeed, pillared by  $\text{L}^2$ . The purity of bulk samples was confirmed via PXRD, and the proposed metal ratios were corroborated via ICP-OES.

Six representative  $\text{M}^1\text{M}^2$ -**RPMs** ( $\text{M}^1$  designates the metal in  $\text{L}^1$  and  $\text{M}^2$  designates the metal in  $\text{L}^2$ ) were synthesized and then analyzed by single crystal X-ray diffraction to confirm their structures. (For **FeMn-RPM**, the structure was disordered near the centers of the dipyriddy struts; see SI.) Each member of this series possesses the same framework with differences only in the identities of the porphyrin metal sites. For Fe- and Mn-porphyrins, the metal center axially ligates a chloride ion to achieve charge balance, while the Al-porphyrin axially ligates a hydroxide ion.

The crystal structures of all materials in the **RPM** series reveal large channels in three directions (see Figure 2) that are occupied



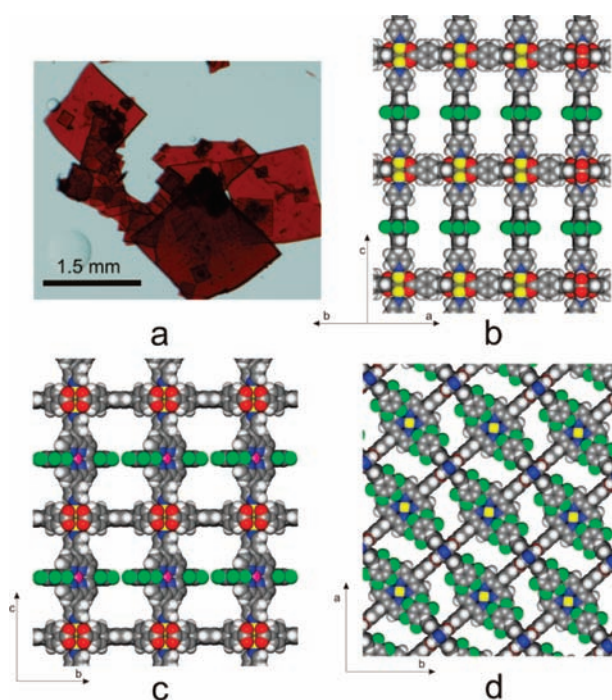


**Figure 3.** (a) Photograph of ZnMn-RPM crystals. (b–d) Space-filling representations of the crystal structure of ZnMn-RPM showing channels in three directions (yellow = Zn, red = O, green = F, blue = N, gray = C, white = H, purple = Mn). Disordered solvent molecules have been omitted.

by a substantial amount of disordered solvents. The metal-to-metal distance between cofacial struts of  $L^1$  is 22 Å, while the distance between cofacial  $L^2$ 's is 16.6 Å. Figure 3 shows a space-filling model of the crystal structure of ZnMn-RPM along the various channels. Importantly, RPMs are composed of a single independent framework (noncatenated), implying a high degree of porosity. This is in stark contrast to the majority of MOF materials, where researchers routinely encounter two- and three-fold catenation, with examples of considerably higher degrees of catenation being known.<sup>23</sup> Noncatenated structures such as obtained for the RPM materials are particularly important for catalytic applications, due to the need for large channels and pores to allow diffusion of reactants into the MOF environment. The immobilization of  $L^1$  and  $L^2$  with large separation distances between the struts should preclude the commonly observed (in homogeneous solution) deactivation of porphyrin-based oxidation catalysts via  $\mu$ -oxo dimer formation.

The hoped-for porosity of the RPM materials was confirmed via TGA measurements, which uniformly revealed 45–60% mass loss due to solvent at  $\sim 110$  °C (Figure S22A). Furthermore, ZnMn-RPM displayed permanent microporosity by gas adsorption ( $\text{CO}_2$  at 273 K); NLDFT analysis provided a surface area of 1000  $\text{m}^2/\text{g}$ . This high porosity is critical for catalysis of reactions involving dissolved species (see below); reagents and substrates that are large (relative to typical gas-phase reactants) must be able to access the metalloporphyrin sites in the pores. All materials exhibited high stability, showing no sign of framework decomposition until 425 °C. Further analysis of a representative framework, ZnMn-RPM, indicates that this material is quite robust and can be resoluted, after solvent removal by heating at 80 °C under dynamic vacuum, with almost no loss of capacity for solvent.

ZnMn-RPM was selected to demonstrate/illustrate the catalytic activity of RPMs containing oxidation catalysts. Using a

soluble analogue of iodosylbenzene, the MOF was found to be an effective catalyst for both the epoxidation of styrene and hydroxylation of cyclohexane. The RPM material showed much greater stability than an analogous homogeneous catalyst. While the homogeneous Mn complex of 5,10,15,20-tetrakis-(pentafluorophenyl)porphyrin showed complete catalyst deactivation after 780 epoxidation turnovers (Figure S24A), ZnMn-RPM functioned for 2150 turnovers, stopping only because of depletion of oxidant. (Figure S24A shows an induction period for catalysis by ZnMn-RPM. This behavior is attributed to slow diffusion of reactants and/or oxidants into the MOF. Consistent with this interpretation, the induction time is considerably shortened when smaller crystallites, obtained by mechanically crushing the crystals, of ZnMn-RPM are used.) No catalytic activity was observed in the reaction solution after removal of the MOF by filtration (in a run where oxidant still remained), confirming that the catalytic reaction is heterogeneous.

Simple filtration and rinsing of the heterogeneous catalyst enabled recovery of the MOF, which was further tested for catalytic activity; the tests revealed activity very similar to that of the initially synthesized material, albeit at roughly two-thirds the earlier rate. (Note that the usual mechanism for catalyst deactivation, oxo-bridged dimer formation, is not available to the framework-constrained porphyrins. We speculate that the decrease in activity instead is due to partial blockage of MOF pores by insoluble polymeric remnants of the consumed oxidant.)<sup>24</sup> In separate experiments, oxidation of cyclohexane proceeded in 20% yield (1 mol % catalyst) to give a mixture of cyclohexanol and cyclohexanone (83:17 alcohol/ketone; see SI).

To check further for permeation of the putatively porous RPMs by reactants such as styrene, we exposed ZnZn-RPM to a chloroform solution of an essentially identically sized compound, 4-vinyl-pyridine (Figure S24B, **1**) that is capable of axially binding to available porphyrinic Zn(II) sites. The test solution also contained the much larger pyridine-functionalized probe molecule, **2** (Figure S24B). Following overnight exposure to an equimolar solution of **1** and **2**, the MOF sample was rinsed repeatedly with chloroform and then digested in aq.  $\text{D}_2\text{SO}_4$ . Consistent with the large size of **2** (i.e., greater than the channel widths in ZnZn-RPM),  $^1\text{H}$  NMR measurements revealed uptake of only trace amounts, presumably present due to binding to Zn(II)porphyrin sites defining the exterior of the MOF. In contrast, the same NMR measurements indicated an extensive uptake of **1**, roughly 60 times that of the control molecule, **2**. Taken together with the TGA experiments described above and the particle-size-dependent induction behavior, these results strongly support the notion that styrene (and cyclohexane) can access the interiors of catalytic RPMs.

In conclusion, we have found that, with the appropriate experimental strategies and design of the organic building blocks, a sizable range of metalloporphyrins can now be incorporated into porous MOFs with retention of open coordination sites necessary for the active-site-based applications for which metalloporphyrins are often used. For example, we have observed that a porous RPM material containing a Mn-porphyrin is catalytically active for routine oxidation reactions, specifically, alkene epoxidation and alkane hydroxylation (albeit, with limited selectivity). The ability to synthesize RPMs from a variety of metalloporphyrin struts opens up possibilities for the design of a wide assortment of porphyrinic MOF materials suitable for catalysis and/or chemical separations. In particular, the ability to incorporate two distinct metalloporphyrins in a single material is highly intriguing as it could enable the synthesis of MOFs containing two distinct catalysts competent to accelerate, sequentially or cooperatively, multiple steps of complex reactions. While the focus

here is mainly on MOF synthesis and characterization, our ongoing work is directed mainly toward new aspects of catalysis.

## ■ ASSOCIATED CONTENT

**S Supporting Information.** Synthesis and characterization of starting materials and MOFs, including single-crystal X-ray diffraction data in CIF format, as well as a detailed description of catalysis conditions. This information is available free of charge via the Internet at <http://pubs.acs.org>.

## ■ AUTHOR INFORMATION

### Corresponding Author

j-hupp@northwestern.edu; stn@northwestern.edu; o-farha@northwestern.edu

## ■ ACKNOWLEDGMENT

We thank Dr. Rebecca Jensen for providing  $L^1$ -Pd. We gratefully acknowledge the NU-ICEP, NU-NSEC, DTRA (Grant HDTRA-09-1-0007), and the AFOSR for financial support. We acknowledge the NU-IMSERC for use of analysis instrumentation. We thank ChemMatCARS and LS-CAT for use of the APS, a facility supported by the U.S. DOE, Office of Science, Office of Basic Energy Sciences (No. DE-AC02-06CH11357). ChemMatCARS Sector 15 is principally supported by the NSF/DOE (NSF/CHE-0822838). Use of the LS-CAT Sector 21 was supported by the Michigan Economic Development Corporation and the Michigan Technology Tri-Corridor (Grant 085P1000817).

## ■ REFERENCES

- (1) (a) Tranchemontagne, D. J.; Mendoz-Cortes, J. L.; O'Keeffe, M.; Yaghi, O. M. *Chem. Soc. Rev.* **2009**, *38*, 1257–1283. (b) Horike, S.; Shimomura, S.; Kitagawa, S. *Nat. Chem.* **2009**, *1*, 695–704. (c) Ferey, G. *Chem. Soc. Rev.* **2008**, *37*, 191–214.
- (2) (a) Allendorf, M. D.; Bauer, C. A.; Bhakta, R. K.; Houk, R. J. T. *Chem. Soc. Rev.* **2009**, *38*, 1330–1352. (b) Murray, L. J.; Dinca, M.; Long, J. R. *Chem. Soc. Rev.* **2009**, *38*, 1294–1314. (c) Li, J.-R.; Kuppler, R. J.; Zhou, H.-C. *Chem. Soc. Rev.* **2009**, *38*, 1477–1504. (d) Hurd, J. A.; Vaidhyanathan, R.; Thangadurai, V.; Ratcliffe, C. I.; Moudrakovski, I. L.; Shimizu, G. K. H. *Nat. Chem.* **2009**, *1*, 705–710. (e) Keskin, S.; Heest, T. M. v.; Sholl, D. S. *ChemSusChem* **2010**, *3*, 879–891. (f) Bradshaw, D.; Claridge, J. B.; Cussen, E. J.; Prior, T. J.; Rosseinsky, M. J. *Acc. Chem. Res.* **2005**, *38*, 273–282.
- (3) (a) Ma, L.; Abney, C.; Lin, W. *Chem. Soc. Rev.* **2009**, *38*, 1248–1256. (b) Corma, A.; Garcia, H.; Xamena, F. X. L. *Chem. Rev.* **2010**, *110*, 4606–4655. (c) Lee, J.-Y.; Farha, O. K.; Roberts, J.; Scheidt, K. A.; Nguyen, S. T.; Hupp, J. T. *Chem. Soc. Rev.* **2009**, *38*, 1450–1459.
- (4) (a) Song, F.; Wang, C.; Falkowski, J. M.; Ma, L.; Lin, W. *J. Am. Chem. Soc.* **2010**, *132*, 15390–15398. (b) Kitaura, R.; Onoyama, G.; Sakamoto, H.; Matsuda, R.; Noro, S.-i.; Kitagawa, S. *Angew. Chem., Int. Ed.* **2004**, *43*, 2684–2687. (c) Cho, S.-H.; Ma, B.; Nguyen, S. T.; Hupp, J. T.; Albrecht-Schmitt, T. E. *Chem. Commun.* **2006**, 2563–2565.
- (5) (a) Wu, C.-D.; Hu, A.; Zhang, L.; Lin, W. *J. Am. Chem. Soc.* **2005**, *127*, 8940–8941. (b) Ma, L.; Falkowski, J. M.; Abney, C.; Lin, W. *Nat. Chem.* **2010**, *2*, 838–846.
- (6) Collman, J. P.; Boulatov, R.; Sunderland, C. J. *Chem. Rev.* **2004**, *104*, 561–588.
- (7) Banerjee, R.; Ragsdale, S. W. *Annu. Rev. Biochem.* **2003**, *72*, 209–247.
- (8) Abrahams, B. F.; Hoskins, B. F.; Michail, D. M.; Robson, R. *Nature* **1994**, *369*, 727–729.
- (9) Shultz, A. M.; Farha, O. K.; Hupp, J. T.; Nguyen, S. T. *J. Am. Chem. Soc.* **2009**, *131*, 4204–4205.
- (10) While it is conceivable that supercritical drying (SCD) could have preserved the porosity of this and other delicate porphyrinic MOFs, it is important to note that the SCD technique has only recently been utilized in the MOF field; see refs 11 and 12.
- (11) (a) Nelson, A. P.; Farha, O. K.; Mulfort, K. L.; Hupp, J. T. *J. Am. Chem. Soc.* **2009**, *131*, 458–460. (b) Cooper, A. I.; Rosseinsky, M. J. *Nat. Chem.* **2009**, *1*, 26–27. (c) Farha, O. K.; Hupp, J. T. *Acc. Chem. Res.* **2010**, *43*, 1166–1175. (d) Bae, Y.-S.; Dubbeldam, D.; Nelson, A. P.; Walton, K. S.; Hupp, J. T.; Snurr, R. Q. *Chem. Mater.* **2009**, *21*, 4768–4777.
- (12) (a) Furukawa, H.; Ko, N.; Go, Y. B.; Aratani, N.; Choi, S. B.; Choi, E.; Yazaydin, A. O.; Snurr, R. Q.; O'Keeffe, M.; Kim, J.; Yaghi, O. M. *Science* **2010**, *329*, 424–428. (b) Farha, O. K.; Yazaydin, A. O.; Eryazici, I.; Malliakas, C. D.; Hauser, B. G.; Kanatzidis, M. G.; Nguyen, S. T.; Snurr, R. Q.; Hupp, J. T. *Nat. Chem.* **2010**, *2*, 944–948. (c) Doonan, C. J.; Morris, W.; Furukawa, H.; Yaghi, O. M. *J. Am. Chem. Soc.* **2009**, *131*, 9492–9493. (d) Xiang, Z.; Cao, D.; Shao, X.; Wang, W.; Zhang, J.; Wu, W. *Chem. Eng. Sci.* **2010**, *65*, 3140–3146. (e) Lohe, M. R.; Rose, M.; Kaskel, S. *Chem. Commun.* **2009**, 6056–6058.
- (13) (a) Kosal, M. E.; Chou, J. H.; Wilson, S. R.; Suslick, K. S. *Nat. Mater.* **2002**, *1*, 118–121. (b) Suslick, K. S.; Bhyrappa, P.; Chou, J. H.; Kosal, M. E.; Nakagaki, S.; Smithenry, D. W.; Wilson, S. R. *Acc. Chem. Res.* **2005**, *38*, 283–291.
- (14) (a) Choi, E. Y.; Barron, P. M.; Novotny, R. W.; Son, H. T.; Hu, C.; Choe, W. *Inorg. Chem.* **2009**, *48*, 426–428. (b) Choi, E. Y.; Barron, P. M.; Novotny, R. W.; Hu, C. H.; Kwon, Y. U.; Choe, W. Y. *CrystEngComm* **2008**, *10*, 824–826.
- (15) Choi, E. Y.; Wray, C. A.; Hu, C. H.; Choe, W. *CrystEngComm* **2009**, *11*, 553–555.
- (16) (a) Lin, K. J. *Angew. Chem., Int. Ed. Engl.* **1999**, *38*, 2730–2732. (b) Goldberg, I. *Chem. Commun.* **2005**, 1243–1254. (c) Pan, L.; Kelly, S.; Huang, X. Y.; Li, J. *Chem. Commun.* **2002**, 2334–2335. (d) Hagrman, D.; Hagrman, P. J.; Zubieta, J. *Angew. Chem., Int. Ed. Engl.* **1999**, *38*, 3165–3168.
- (17) Barron, P. M.; Wray, C. A.; Hu, C.; Guo, Z.; Choe, W. *Inorg. Chem.* **2010**, *49*, 10217–10219.
- (18) The substantial (but not complete) degradation of crystallinity following solvent evacuation (as indicated by powder measurements) and anomalously low values for solvent loss as measured by thermogravimetric analysis (ca. 15 to 10 wt % observed, ca. 65 wt % expected, see ref 17) likewise are suggestive of framework collapse. It is conceivable that collapse can be avoided by modifying the MOF activation protocol.
- (19) Only ZnZn-RPM was examined. While the measured surface area is less than expected from the material's crystal structure, it should be noted that the detailed activation protocol was not optimized; see SI. For a discussion of the application of NLDFT to CO<sub>2</sub> isotherms, for the assessment of surface area, see: Jagiello, J.; Thommes, M. *Carbon* **2004**, *42*, 1227–1232.
- (20) Alkordi, M. H.; Liu, Y.; Larsen, R. W.; Eubank, J. F.; Eddaoudi, M. *J. Am. Chem. Soc.* **2008**, *130*, 12639–12641.
- (21) (a) Sheldon, R. A. *Metalloporphyrins in Catalytic Oxidations*; Marcel Dekker, Inc.: New York, 1994. (b) Meunier, B. *Chem. Rev.* **1992**, *92*, 1411–1456.
- (22) (a) Farha, O. K.; Mulfort, K. L.; Hupp, J. T. *Inorg. Chem.* **2008**, *47*, 10223–10225. (b) Farha, O. K.; Malliakas, C. D.; Kanatzidis, M. G.; Hupp, J. T. *J. Am. Chem. Soc.* **2010**, *132*, 950–952.
- (23) (a) Batten, S. R. *CrystEngComm* **2001**, *3*, 67–72. (b) Gadzikwa, T.; Zeng, B.-S.; Hupp, J. T.; Nguyen, S. T. *Chem. Commun.* **2008**, 3672–3674.
- (24) 1 mg of catalyst (the amount typically used) produces nearly 400 mg of depleted oxidant. The depleted oxidant readily aggregates to form an insoluble polymer. An additional 400 mg of insoluble polymer is formed via spontaneous degradation of the oxidant (and thus requiring the oxidant to be used in ca. 2-fold excess).